



Influence of Barrel Vibration on the Barrel Muzzle Position at the Moment when Bullet Exits Barrel

M. Štiavnický and P. Lisý*

Department of Mechanical Engineering, Academy of the Armed Forces, Liptovský Mikuláš, Slovak Republic

The manuscript was received on 28 March 2012 and was accepted after revision for publication on 12 February 2013.

Abstract:

By numerical simulation, influence of the barrel fixing on barrel vibration when a bullet moves down the barrel during shot will be investigated. Both the barrel and bullet were modelled by LS-DYNA software. The barrel is modelled as perfectly straight without any manufacturing deviations. The bullet is a NATO standard 5.56mm calibre consisting of brass jacket and lead core. Gas pressure is applied on the barrel and bullet base. As the bullet is forced into the lands of the barrel, the bullet obtains forward momentum and rotational speed. Interaction of the bullet with the barrel acts as excitation force and the barrel vibrates. In this article, two modifications of the barrels with and without the attachments are shown. These all have an influence on the barrel behaviour during shot mainly at the moment when the bullet leaves the barrel muzzle. Also some impulses are given to the barrel when the bullet leaves the barrel muzzle.

Keywords:

Assault rifle, barrel vibration, numerical simulation

1. Introduction

There are not many articles on accuracy of the small arms from the point of view of the barrel vibration. For very short firing distances the vibration of the barrel can as well be neglected, nonetheless this is still important for the precision of a shot on long range. There are many variables which affect the accuracy of a weapon [1-3]. Mainly these are the manufacturing tolerances, such as the straightness of the barrel bore, uniformity of the geometry of the barrel, the variations in the width of lands and in the depth of grooves and also the surface finish. It is shown in [4, 5] that for the large

* Corresponding author: Department of Mechanical Engineering, Academy of the Armed Forces of Gen. M. R. Štefánik, Demänová 393, 031 06 Liptovský Mikuláš, Slovak Republic, phone: +421 960 423357, e-mail: peter.lisy@aos.sk

calibre systems the vibrations arising from the imperfections of the barrel play a major role in flight path of the bullet. These influences will be intentionally neglected in this article to show the extent of the vibrations arising from the dynamics of the barrel-bullet system for the initially perfect internal conditions.

When a weapon is fired, there are vibrations induced in the steel barrel as the bullet moves down it. If the barrel is fixed into a weapon case or butt-stock (which may be made of wood, metal or plastics) in an improper length, the barrel vibrations are damped differently. That means that the point where the bullet strikes will be changed. In dependency where the butt-stock (or weapon case in case of bull pup system) is leant onto the arm and how loosely or tightly the pistol grips is the fixing may also affect the vibration damping characteristics and thereby the accuracy of the weapon. The same thing happens when some accessories are put on the barrel (e.g. muzzle devices as a muzzle compensator, a silencer, a muzzle attachment for foresight or an attachment for a gas piston etc., see Fig. 1). The paper [6] shows the variation of natural frequencies versus modes with modification in fixing the free-floated barrel where there is no contact between the barrel and anything else and also when on the barrel the muzzle compensator for three different barrels is attached. In this article, we will investigate by numerical simulation what influence has the barrel fixing on the barrel vibration (mainly on its muzzle), when the bullet is moving down the barrel during shot. Apart from this, a situation will be investigated when some accessories will be set on the barrel.



Fig. 1 Barrel and some of its accessories [7]

A complete nonlinear analysis is performed for each barrel modification, as it is not known beforehand how the nonlinear system will behave after changing some conditions. The system could be modelled as linear to investigate only the natural frequencies. For purposes of this article, a nonlinear approach has been chosen where the excitation of the barrel is caused not only by the pressure distribution in the barrel, but also by the interaction of the bullet with the barrel. Even though the bullet is modelled as geometrically perfect with no deviations in mass and shape, it has also been assigned plastic properties. This means that as the bullet is forced into the barrel rifling, it deforms permanently and some imperfections are created. The changes in the mass distribution of the bullet and its shape variations are caused by further excitation of the barrel. The aim of the article is to investigate the vibration of the barrel during shot in its complexity, including the interaction of the bullet with the barrel. But we are interested only in the internal accuracy of the weapon, i.e. the accuracy that can be affected by modifications in the design and construction of the weapon itself. There are also external influences, such as variations in the outer environment, variations in bullet shape and weight and variations in the propellant weight and its thermo-mechanical properties and many others which cannot be influenced directly. As we are interested in the design and construction optimization of the weapon to achieve the best internal accuracy, the external influences are neglected.

2. Method of Solution

In standard three-dimensional case for dynamic analysis, the problems are described by harmonic equation containing spatial derivatives of an unknown function θ as follows [8]:

$$\frac{\partial}{\partial x} \left(k \frac{\partial \theta}{\partial x} \right) + \frac{\partial}{\partial y} \left(k \frac{\partial \theta}{\partial y} \right) + \frac{\partial}{\partial z} \left(k \frac{\partial \theta}{\partial z} \right) = \rho \frac{\partial^2 \theta}{\partial t^2} + c \frac{\partial \theta}{\partial t} - Q, \quad (1)$$

where k is the stiffness of the structure, Q is the external load applied to the structure and c and ρ are the damping and mass density properties of material respectively. The unknown function is a function of space coordinates and of time whereas the structural and material properties are the functions of space, time and also the functions of the unknown quantity for nonlinear problems. In order to solve such equation by numerical means, it is required for the problem to be discretized onto finite elements that means space discretization where the unknown quantity in any point in the structure domain can be approximated as:

$$\theta = \sum N_i u_i = \mathbf{N} \mathbf{u}, \quad (2)$$

where N_i is the shape functions from the nodal values u_i .

The linear brick elements were used in the model with corresponding linear shape functions [9]:

$$N_i = \frac{1}{8} (1 + \xi \xi_i) (1 + \eta \eta_i) (1 + \zeta \zeta_i), \quad (3)$$

where ξ , η , ζ denotes the local coordinate system and ξ_i , η_i , ζ_i are the natural coordinates of i -th node. One-point Gauss integration was performed for constant stress in element volume.

Denoting the right side in Eq. (1) by p , the total force acting on the structure can be derived using the shape functions as:

$$\mathbf{p} = \int_V \mathbf{N}^T \left(\rho \frac{\partial^2 \theta}{\partial t^2} + c \frac{\partial \theta}{\partial t} - Q \right) dV. \quad (4)$$

Further, according to Eq. (2), the unknown variable θ can be approximated in terms of the nodal values \mathbf{u} :

$$\mathbf{p} = \left(\int_V \mathbf{N}^T \rho \mathbf{N} dV \right) \frac{d^2 \mathbf{u}}{dt^2} + \left(\int_V \mathbf{N}^T c \mathbf{N} dV \right) \frac{d\mathbf{u}}{dt} - \int_V \mathbf{N}^T Q dV. \quad (5)$$

The left side of the Eq. (1) leads to a formulation of the stiffness matrix in terms of the shape function derivations which are expressed as a strain matrix \mathbf{B} :

$$\mathbf{B} = [\mathbf{B}_1 \quad \mathbf{B}_2 \quad \mathbf{B}_3 \quad \mathbf{B}_4 \quad \mathbf{B}_5 \quad \mathbf{B}_6 \quad \mathbf{B}_7 \quad \mathbf{B}_8], \quad (6)$$

where

$$\mathbf{B}_i = \begin{bmatrix} \frac{\partial N_i}{\partial x} & 0 & 0 & 0 & \frac{\partial N_i}{\partial z} & \frac{\partial N_i}{\partial y} \\ 0 & \frac{\partial N_i}{\partial y} & 0 & \frac{\partial N_i}{\partial z} & 0 & \frac{\partial N_i}{\partial x} \\ 0 & 0 & \frac{\partial N_i}{\partial z} & \frac{\partial N_i}{\partial y} & \frac{\partial N_i}{\partial x} & 0 \end{bmatrix}^T. \quad (7)$$

Thus the stiffness matrix \mathbf{K} can be formulated, and also the mass matrix \mathbf{M} and the damping matrix \mathbf{C} are obvious from previous calculations, as is the external force vector \mathbf{f} :

$$\begin{aligned} \mathbf{K} &= \int_V \mathbf{B}^T \mathbf{D} \mathbf{B} dV \\ \mathbf{M} &= \int_V \mathbf{N}^T \rho \mathbf{N} dV \\ \mathbf{C} &= \int_V \mathbf{N}^T c \mathbf{N} dV, \\ \mathbf{f} &= \int_V \mathbf{N}^T Q dV \end{aligned} \quad (8)$$

where \mathbf{D} is the material constants matrix for isotropic material:

$$\mathbf{D} = \begin{bmatrix} \frac{E(1-\nu)}{(1-2\nu)(1+\nu)} & \frac{E\nu}{(1-2\nu)(1+\nu)} & \frac{E\nu}{(1-2\nu)(1+\nu)} & 0 & 0 & 0 \\ \frac{E\nu}{(1-2\nu)(1+\nu)} & \frac{E(1-\nu)}{(1-2\nu)(1+\nu)} & \frac{E\nu}{(1-2\nu)(1+\nu)} & 0 & 0 & 0 \\ \frac{E\nu}{(1-2\nu)(1+\nu)} & \frac{E\nu}{(1-2\nu)(1+\nu)} & \frac{E(1-\nu)}{(1-2\nu)(1+\nu)} & 0 & 0 & 0 \\ 0 & 0 & 0 & G & 0 & 0 \\ 0 & 0 & 0 & 0 & G & 0 \\ 0 & 0 & 0 & 0 & 0 & G \end{bmatrix} \quad (9)$$

and E , ν and G are Young's modulus, Poisson's ratio and shear modulus respectively.

Finally the Eq. (1) can be assembled in the matrix form which gives differential equation for dynamic motion:

$$\mathbf{M}\ddot{\mathbf{u}} + \mathbf{C}\dot{\mathbf{u}} + \mathbf{K}\mathbf{u} = \mathbf{f}, \quad (10)$$

where the dot signifies temporal derivation. The temporal discretization is solved by forwarding the solution from initial conditions by central difference method. It means that as soon as the accelerations are known, the velocity and displacement are stepped using the values from the last step as follows:

$$\begin{aligned} v_{i+1/2} &= v_{i-1/2} + a_i \Delta t_i \\ u_{i+1} &= u_i + v_{i+1/2} \Delta t_{i+1/2}, \end{aligned} \quad (11)$$

where

$$\Delta t_{i+1/2} = \frac{\Delta t_i + \Delta t_{i+1}}{2}, \quad (12)$$

updating all nodal values in the i -th cycle.

3. Numerical Simulation by LS-DYNA

To solve the problem which is stated in the introduction, the FEM software has been used to create 3-D models of the barrel and bullet (Fig. 2) in the LS-DYNA program [10]. The model has globally 58,052 8-node hexahedral solid elements and 65,824 nodes. The interaction between the barrel bore and bullet is done through the surface to surface contact of the active segments. The barrel was created for the NATO 5.56 mm cartridge and a bore has six lands and six grooves, with twist rate of rifling 1:9. The bullet was created with the bullet core made of Pb-Sn and jacket made of brass. We can see correctness of the created model in Fig. 3, where the engraving of the land on the bullet jacket is shown. In Fig. 3 the model of the barrel with two rings is also shown, which represents the places (at the barrel muzzle and half of the barrel) and the weight of some accessories, which were added on the barrel. The bullet base is at the barrel muzzle at time 0.7765 ms. To this time in Tab. 1 there are listed the results of displacements in directions x , y , z and also values of resultant accelerations which are occurring. All listed data refer to node 10648, which is the last node on the land at the barrel muzzle in the direction of y -axis above the centre of bore (Fig. 3). These results were obtained by a simulation of two kinds of barrels (cylindrical and cone-shaped) at three different fixing lengths (20 mm, 40 mm and 60 mm) and for three different added weights (1 – 5 × 20, 2 – 5 × 20 twice, 3 – 10 × 30, all dimensions are in mm). The cone-shaped barrel is quite close to the real barrel, i.e. its length is 488 mm, a part around the barrel chamber is cylindrical and the next part to the muzzle is conical. The time dependence of the pressure in the barrel bore was applied as a curve which was obtained by a ballistic measurement of the NATO 5.56mm cartridge.

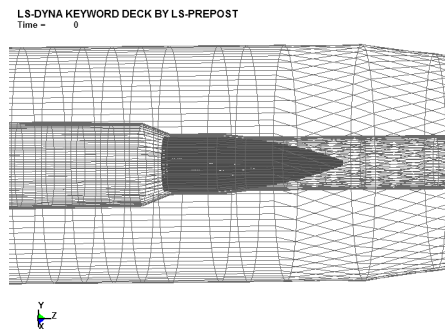


Fig. 2 Part of finite element model of barrel and bullet (at time of simulation 0 ms)

Table 1 illustrates the results of FEA analysis of displacements and acceleration at node 10648 on the barrel muzzle, as well as the displacements at the node 26703 which is in the centre of the bullet base. All results are detached on the initial centre of the bore. Two kinds of the barrels have been investigated. Each one of them was investigated itself, without any accessory at three different fixing lengths; each of them was modified by the additional accessory or accessories. The accessories have to simulate additional weight, which is added on the barrel muzzle, e.g. a foresight,

a bayonet etc. Also in the half of the barrel (Fig. 3) or closer to the muzzle (Fig. 1) has also been put an additional weight for a gas piston for extraction of gases. We can designate all accessories which are possible to be added on the barrel today. We can here compare the results for each barrel itself. Consequently, we can see the differences between the fixing lengths of the barrels, which have an influence on the position of the muzzle when the bullet flies out from the barrel. Also in Table 1, displacements of the barrel muzzle in x , y , z -axis during shot, when the barrel is stressed by the action of gas pressure and motion of the bullet, are shown.

Tab. 1 Results of displacements and acceleration at node 10648 and displacements bullet at node 26703 on the barrel muzzle when bullet flies out from the barrel muzzle

Barrel (Accessories)	Fixing [mm]	Displacement node 10648			Resultant acceleration Node 10648	Displacement node 26703	
		x	y	z		x	y
		$\times 10^3$ [mm]	$\times 10^3$ [mm]	$\times 10^3$ [mm]	$\times 10^{-3}$ [mm/ms ²]	$\times 10^3$ [mm]	$\times 10^3$ [mm]
Cylindrical	20	-6.86	8.89	-3.24	26.38	-0.41	1.31
Cylindrical	40	-4.33	6.56	-0.97	29.47	19.17	-10.75
Cylindrical	60	-6.27	8.42	0.099	51.69	-7.11	8.55
Cylindrical (1)	20	-6.22	12.30	-3.89	162.95	1.40	0.31
Cylindrical (1)	40	-5.50	6.01	-1.81	28.13	1.33	1.83
Cylindrical (1)	60	-5.84	14.89	-1.32	76.53	-2.69	13.49
Cylindrical (2)	20	-5.20	5.62	-4.55	115.96	-4.72	-10.67
Cylindrical (2)	40	-5.16	12.40	-2.37	8.19	-4.38	-24.75
Cylindrical (2)	60	-5.08	5.46	-2.02	19.32	-2.32	-7.10
Cylindrical (3)	20	-5.02	10.29	-2.95	17.64	-2.71	4.69
Cylindrical (3)	40	-6.87	8.45	-3.34	21.50	-10.27	-7.22
Cylindrical (3)	60	-4.42	5.87	-1.32	167.89	0.34	26.04
Cone-shaped	20	-6.98	7.42	4.30	67.32	7.97	6.85
Cone-shaped	40	-7.33	9.41	4.38	47.26	5.30	8.51
Cone-shaped	60	-5.36	3.71	3.69	41.70	-4.50	3.95
Cone-shaped (1)	20	-6.29	9.18	1.35	140.00	-10.08	-7.23
Cone-shaped (1)	40	-4.32	7.42	3.20	110.76	20.10	-3.35
Cone-shaped (1)	60	-2.66	9.07	0.49	32.34	1.42	-2.57
Cone-shaped (2)	20	-5.95	9.15	-1.51	92.17	-8.08	0.95
Cone-shaped (2)	40	-5.94	9.37	2.24	14.49	-7.18	1.52
Cone-shaped (2)	60	-6.18	8.80	-0.61	12.421	6.38	4.53
Cone-shaped (3)	20	-5.06	5.30	-5.33	101.21	-4.56	1.96
Cone-shaped (3)	40	-3.26	7.93	-4.13	81.13	12.49	-2.54
Cone-shaped (3)	60	-5.83	11.60	-1.33	6.58	10.46	2.90

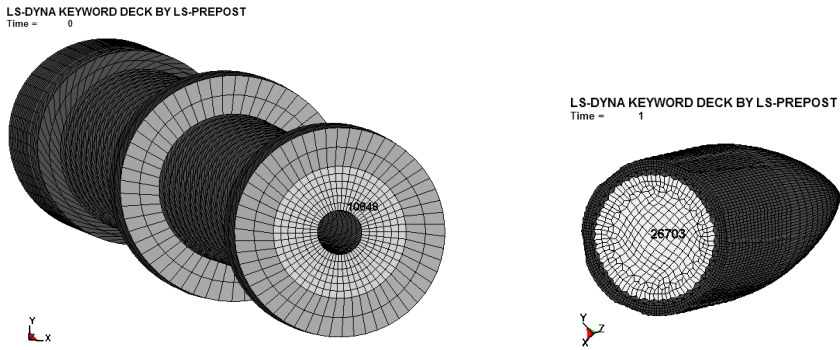


Fig. 3 Cone-shaped barrel (2) and bullet at the time of simulation 1 ms

From Figs 4 to 7 it is also evident that the largest displacements of the barrel occur in the beginning of the bullet motion where is the area of the maximum pressure and area of the engraving the bullet to the grooved bore of the barrel.

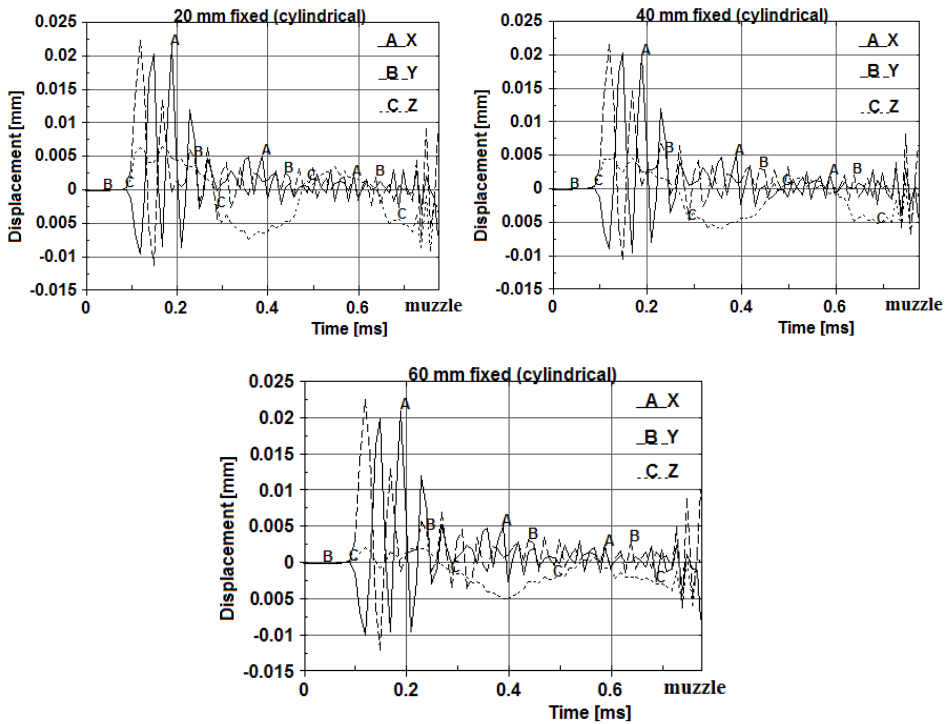


Fig. 4 Displacement of the barrel muzzle of the cylindrical barrel at node 10648 in x, y, z-axis at three different fixing length

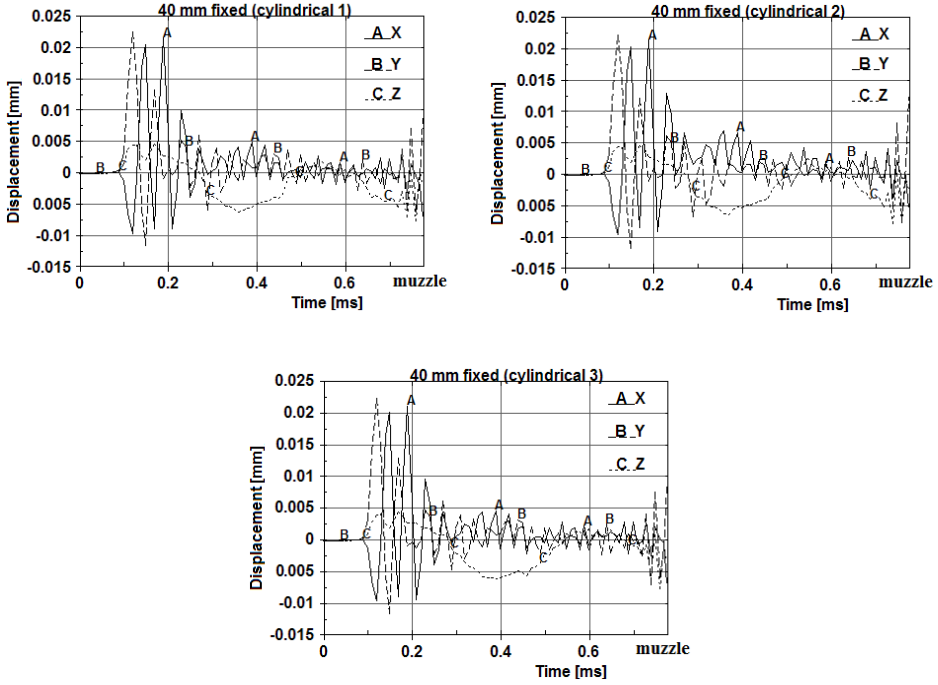


Fig. 5 Displacement of the barrel muzzle of the cylindrical barrel at node 10648 in x, y, z-axis at 40 mm fixing with added weight 1, 2, 3

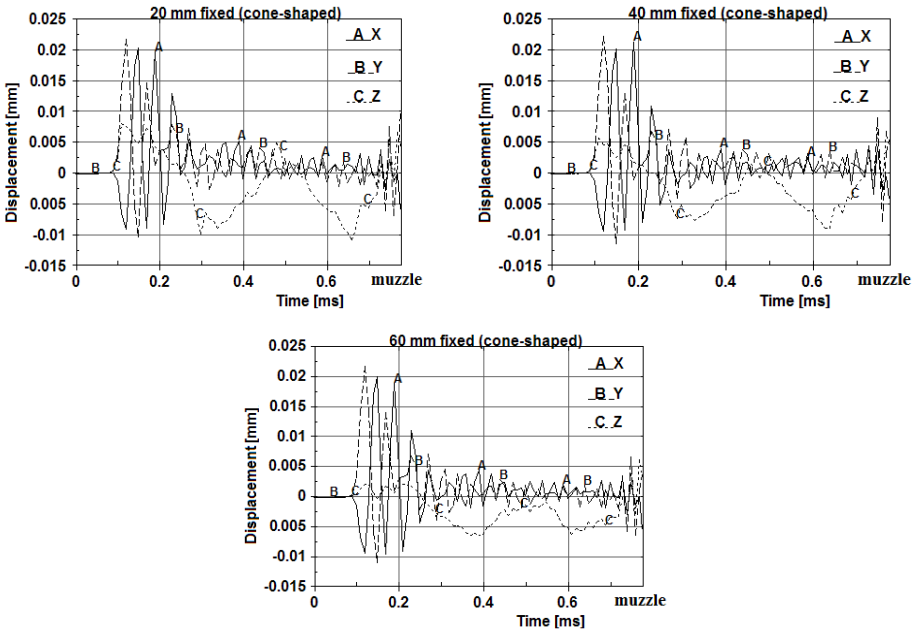


Fig. 6 Displacement of the barrel muzzle of the cone-shaped barrel at node 10648 in x, y, z-axis at three different fixing lengths

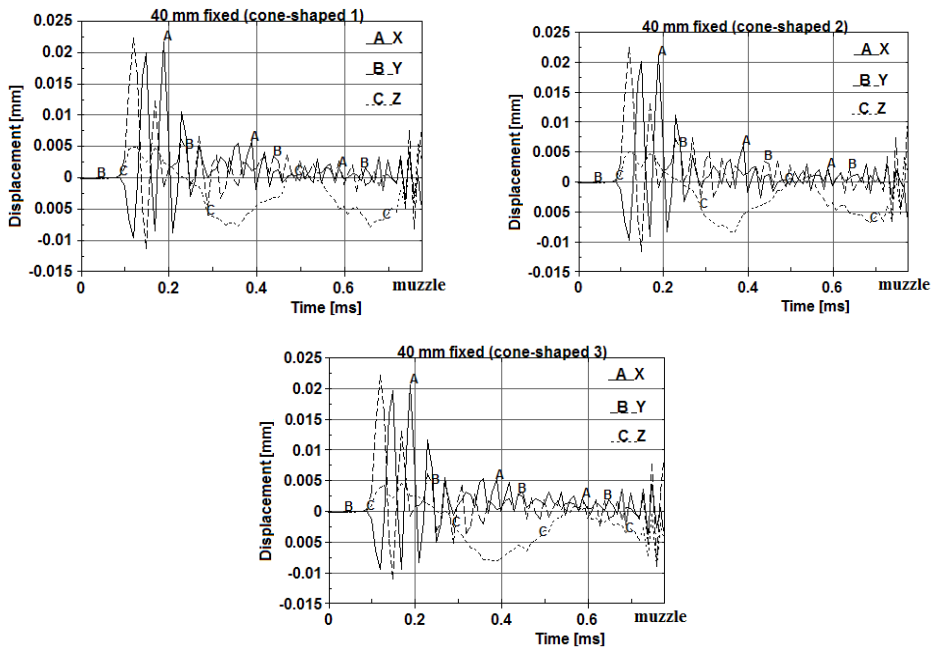


Fig. 7 Displacement of the barrel muzzle of the cone-shaped barrel at node 10648 in x, y, z-axis at 40 mm fixing with added weight 1, 2, 3

Moreover, the results of resultant acceleration of the node 10648 when the bullet leaves the barrel muzzle are shown here. The resultant acceleration in the barrel muzzle is the biggest when the bullet leaves the barrel muzzle (Fig. 8 and 9). This excites the barrel to vibration which can have an influence on the next shot.

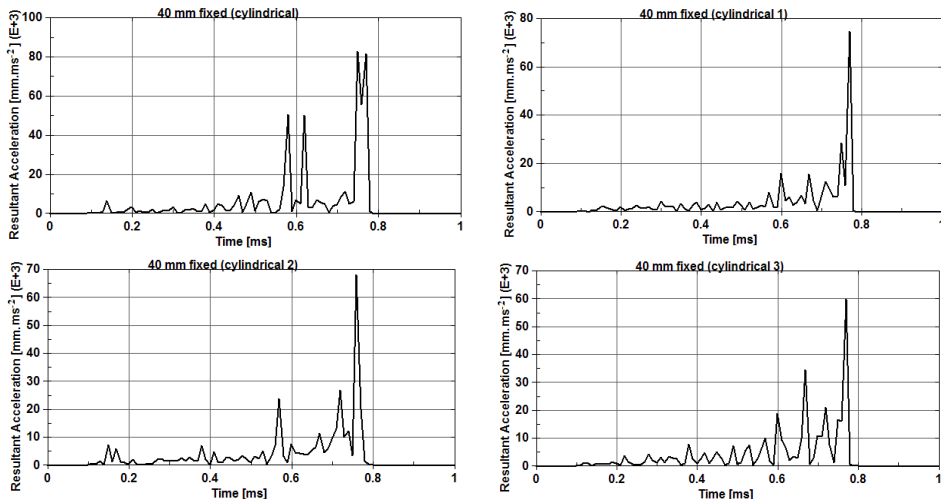


Fig. 8 Resultant acceleration of the barrel muzzle of the cylindrical barrel at node 10648 at 40 mm fixing without and with added weight 1, 2, 3

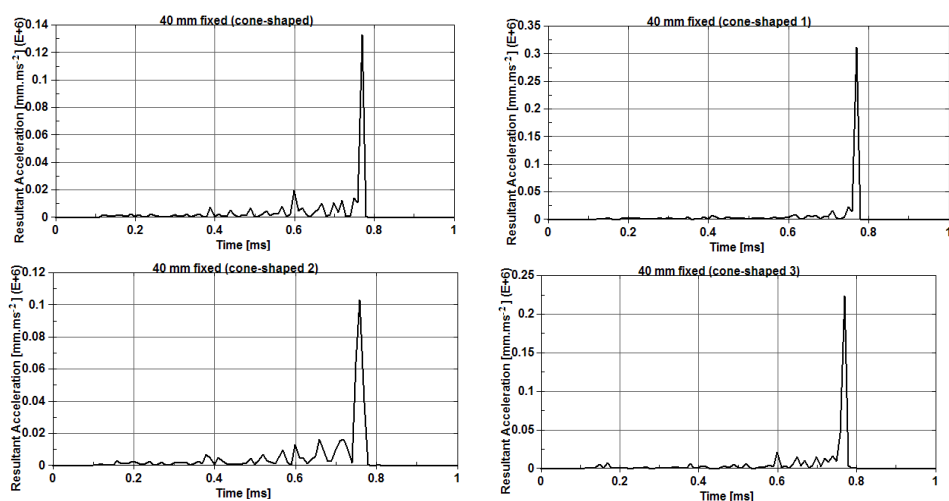


Fig. 9 Resultant acceleration of the barrel muzzle of the cone-shaped barrel at node 10648 at 40 mm fixing without and with added weight 1, 2, 3

From Table 1 the coordinates in x-axis and y-axis for the bullet at node 26703 (Fig. 3) when the bullet leaves the barrel muzzle are also evident. These coordinates are not zero although axis of the barrel and bullet are axially symmetrical at simulation, which means that they have not produced deviations. Because the barrel during shot is excited, as was stated earlier, therefore coordinates in x and y-axis are not zero. This is clearly apparent from Figs 10 to 12 for chosen examples where are shown courses of the bullet during shot at the barrel and its position at the barrel muzzle when the bullet leaves the barrel. We can see differences between Fig. 10 and Fig. 11 where the same barrels were taken, but with a different fixing length. Accordingly, the differences are evident from Fig. 12, although the cone-shaped barrels have the same fixation, but they have been added different accessories.

The differences are more evident from Figs 13 to 16, where a flight of the bullet from the barrel is shown at certain time outside of the barrel for the chosen barrels. Also the bullet is affected by the barrel vibration and when the bullet leaves the barrel muzzle, the bullet base is pushed off the initial centre of bore and the bullet starts to yaw. It can be seen that due to the centrifugal force as the bullet spins with high rotational velocity, the bullet is stabilized after some time, but is already pointing off the initial centre of bore. The direction and magnitude of the bullet yaw are dependent on various combinations of fixing lengths of the barrel and additional accessories. This dispersion of the bullet courses is due to only the initially perfect internal conditions of the barrel-bullet system. Regarding of this it might be of benefit to tune the barrel in a way that the node of the vibration of the barrel will be precisely located at the muzzle. The result of this modification can be in smaller impulse to the bullet and the shot would be more accurate.

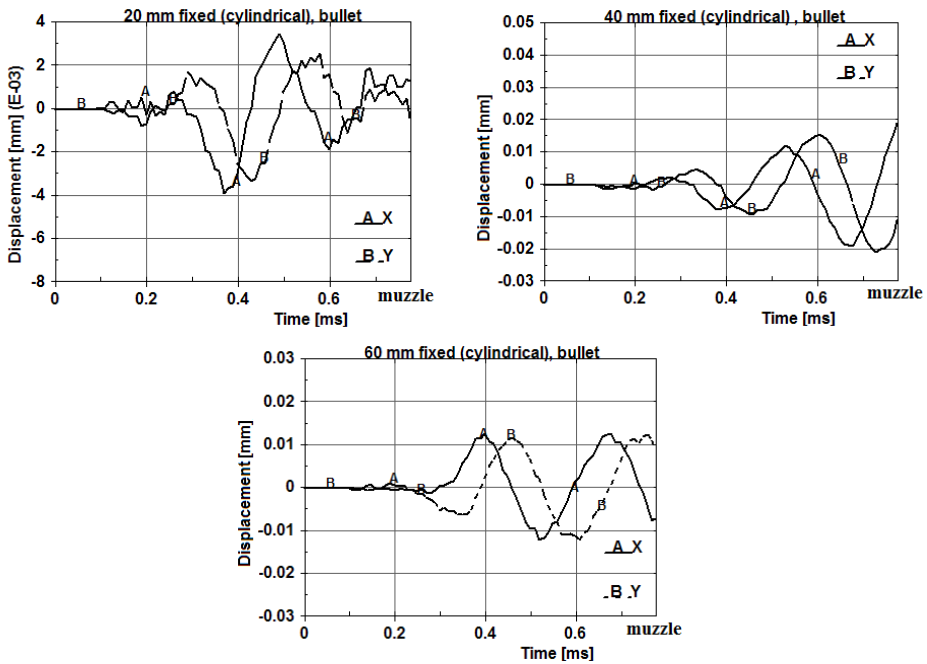


Fig. 10 Displacement of bullet at node 26703 at the barrel muzzle of the cylindrical barrel in x, y-axis at three different fixing lengths

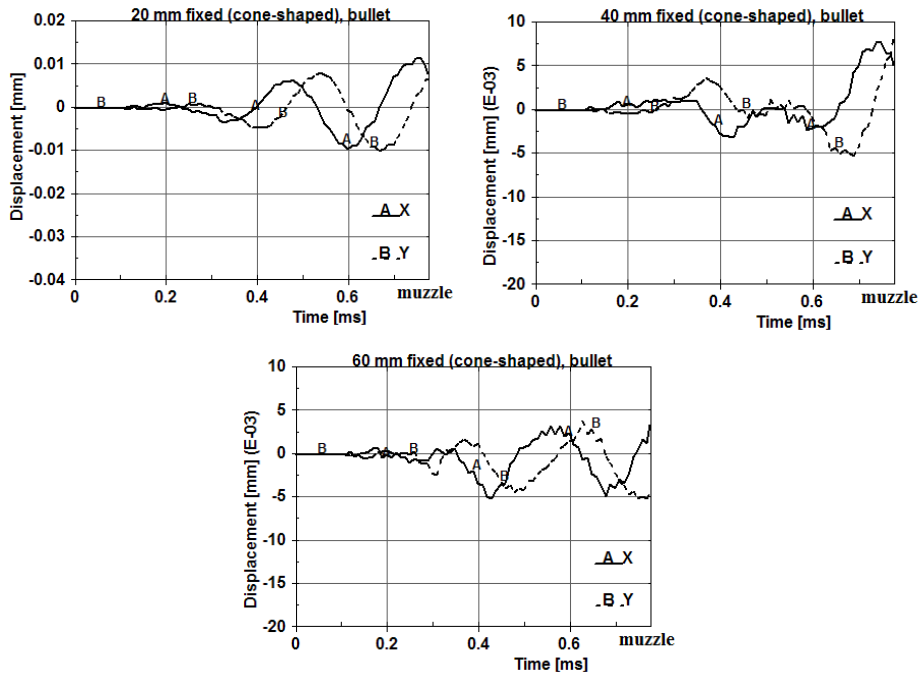


Fig. 11 Displacement of bullet at node 26703 at the barrel muzzle of the cone-shaped barrel in x, y-axis at three different fixing lengths

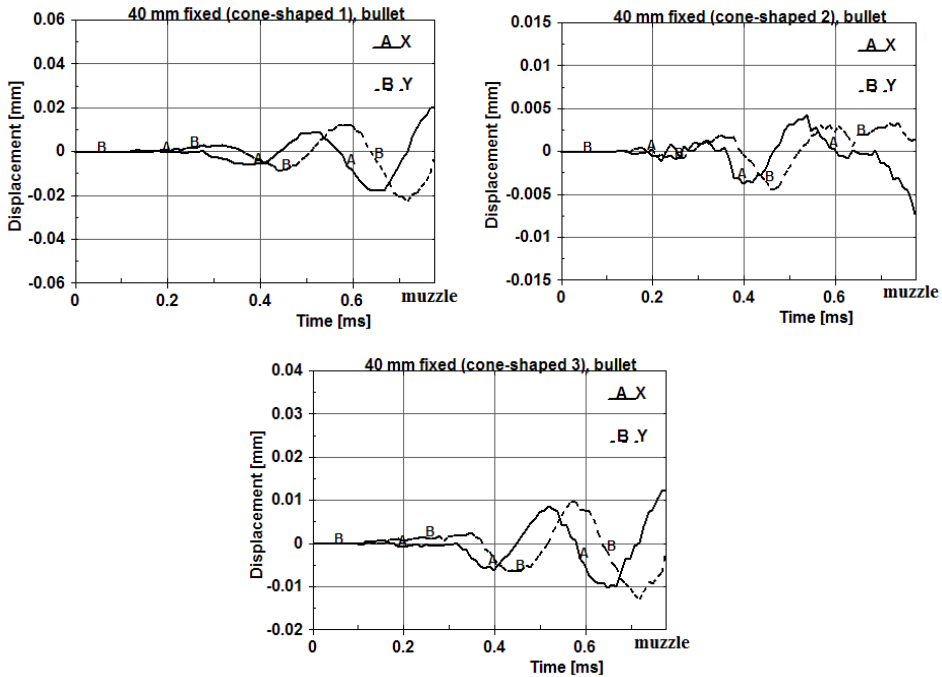


Fig. 12 Displacement of bullet at node 26703 at the barrel muzzle of the cone-shaped barrel in x, y-axis at 40 mm fixing with added weight 1, 2, 3

4. Conclusion

This article presents the simulation of the influence of different fixing of the barrels to the weapon case for two different barrels (cylindrical and cone-shaped) with and without added accessories when were applied both the gas pressure and motion of the bullet inside the barrel. In Table 1 and Figs 4 to 9, we can see the behaviour of the muzzle barrel at node 10648 during shot for the chosen samples. The corresponding values are shown in the table, categorically ordered for all combinations of the barrel fixing length and accessories that were considered. Also here was investigated the influence of the barrel vibration during shot on the position of the barrel muzzle at the moment when the bullet exits the barrel and how this is affecting the direction of the bullet flight. From Figs 10 to 16 it is evident that the bullet is yawing due to the interaction with the barrel muzzle in the moment when it leaves the muzzle. The model is fairly accurate and the bullet flight is stabilized after few moments because of gyroscopic effect. The results presented here are valid for the perfect initial internal conditions, the barrel is perfectly straight and the bullet is initially aligned with the barrel axis. This was done on the purpose to separate the forced vibration due to loading. The effects of the barrel vibrations should be even more dramatic in real conditions. Shot accuracy might be increased by directing the node of the vibration at the muzzle. This might be investigated in the future research.

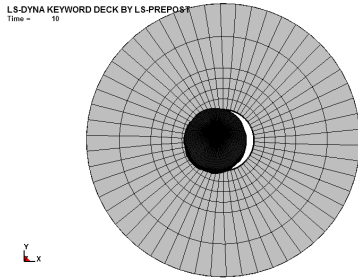


Fig. 13 Cylindrical barrel at fixing 40 mm, deviation at 10 ms fly time of bullet

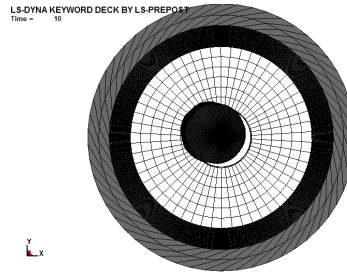


Fig. 14 Cone-shaped barrel at fixing 40 mm, deviation at 10 ms fly time of bullet

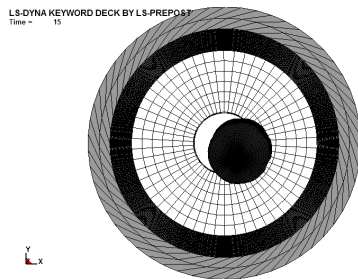


Fig. 15 Cylindrical barrel at fixing 60 mm, deviation at 15 ms fly time of bullet

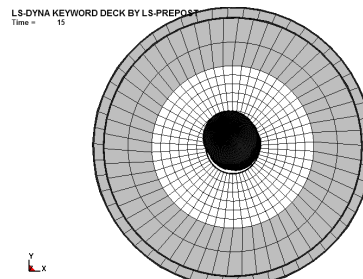


Fig. 16 Cone-shaped barrel at fixing 40 mm, deviation at 15 ms fly time of bullet

References

- [1] LILJA, D. *What Makes a Rifle Barrel Accurate?* [on line]. [cited 2012-03-14] Available from: <http://www.riflebarrels.com/articles/barrel_making/rifle_barrel_accurate.htm>.
- [2] VÍTEK, R. Influence of the small arm barrel bore length on the angle of jump dispersion. In *Proceedings of the 7th WSEAS International Conference on System science and simulation in engineering ICOSSE'08*. Wisconsin: WSEAS, 2008, p. 114-118. ISBN 978-960-474-027-7.
- [3] PROCHÁZKA, S., SEMAN, P. and VÍDEŇKA, M. Deformation of the Cannon Barrel when Projectile Goes by Muzzle. In *Proceedings of 9th Symposium on Weapon Systems*. Brno: University of Defence, 2009, p. 43-49.
- [4] ECHES, N. et al. Modelling of the dynamics of a 40 mm gun and ammunition system during firing. In *Proceedings of 7th European LS-DYNA conference*. Salzburg: DYNAmore, 2009.
- [5] ECHES, N et al. In bore behaviour of large calibre armour piercing fin stabilized discarding sabot projectiles. In *Proceedings of 20th International Symposium on Ballistics*. Orlando (Florida): ISL, 2002.

- [6] LISÝ, P., ŠTIAVNICKÝ, M. Modal Analysis of Barrels for Assault Rifles. In *Proceedings of 8th International Armament Conference on Scientific Aspects of Armament & Safety Technology* (October 6-8, 2010, Pultusk). Warsaw: Military University of Technology, 2010, p. 135.
- [7] *SIG SG 550 assault rifle* [on line]. [cited 2012-03-14] Available from: <http://en.wikipedia.org/wiki/SIG_SG_550>.
- [8] *LS-DYNA: Theory manual, version 971*. Livermore (California): Livermore Software Technology Corporation, 2007.
- [9] BATHE, KJ. et al. *Finite Element Procedures*. New Jersey: Prentice Hall Inc., 1996. 1037 p.
- [10] *LS-DYNA: Keyword user's manual, version 971*. Livermore (California): Livermore Software Technology Corporation, 2007.